

THE IMPACT OF TUNGSTEN LONG ROD PENETRATORS INTO WATER FILLED TARGETS

Leonard T. Wilson (1), David L. Dickinson (1), Eugene S. Hertel, Jr. (2)

(1) Naval Surface Warfare Center Dahlgren Division, Dahlgren, VA

(2) Sandia National Laboratories, Albuquerque, NM

Twelve experiments were conducted to determine the effect of water filled targets on the penetration of tungsten long rods in terms of their residual mass and integrity. CTH hydrocode calculations were performed for each of the experiments to ensure that the erosion and breakup of the tungsten projectiles could be accurately reproduced. The CTH hydrocode predictions correlate well with the experimental results in most cases. Only 8% of the variance is unexplained. The slip interface between the rod and water was approximated in one of two ways, 1) using the CTH BLINT option in 2-D or 2) using a standard Eulerian mixed cells treatment. Results indicate that a 3-D BLINT algorithm is critical to predicting rod residual lengths. We were unable to reproduce rod fracture that occurred in every experiment where the water column exceeded 25 cm in length. We feel that this is due to a change in rod material properties during penetration, and continue to investigate the issue.

BACKGROUND

The late Dr. Andrew Williams conducted a series of rod impact experiments at the Naval Research Laboratory (NRL). In these experiments, tungsten long rod penetrators were launched against water filled targets. The objective was to determine the effect of the water filled targets on the penetrators in terms of their residual mass and integrity. The experimental data from these tests will be used to enhance the capabilities of the FATEPEN2 engineering code that is used to predict fragment and projectile penetration [1].

There were two experimental configurations. The first, shown in figure 1, consisted of a length of PVC pipe filled with water and capped with plexiglass [2]. Nine experiments were performed using this water column configuration. Rod length to diameter ratios ranged from 3 to 15 in these experiments, while impact velocities ranged from 2.26 to 4.57 km/s.

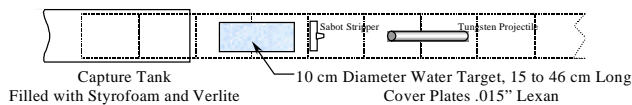


Figure 1. Water Filled Cylinder Experiment

The second configuration, shown in Figure 2, consisted of four tanks of water, oriented so that the angle between the penetrator and wall varied between 13 and 45°.

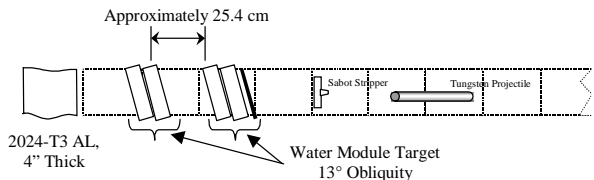


Figure 2. Water Module Experimental Set-up

As can be seen, there are approximately 25.4 cm between the first and second set of tanks. There were three experiments performed using this water module configuration. Rod length to diameter ratios varied from 25 to 38, and impact velocities were in the 2.25 km/s range. Flash radiography was used in all twelve experiments to track the rods as they penetrated the water.

To support this project, calculations using the CTH hydrocode were performed for each experiment [3]. These calculations were made using platforms ranging from individual workstations to massively parallel computer systems resident at Sandia National Laboratories (SNL). The purpose of this companion effort was to provide insight into the experimental results.

Our goals in this paper are to summarize the experiments performed and their corresponding calculations, providing a quantitative comparison between the two. We will first summarize the twelve experiments. We will then describe the approach taken in the numerical analysis. Following this discussion, we will correlate the results of the experiments and the CTH calculations, and provide insight into any discrepancies. We will end by presenting relevant conclusions.

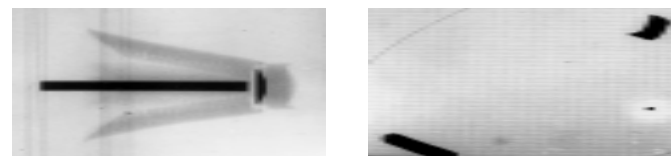
EXPERIMENTAL RESULTS

The nine water column experiments are summarized below in Table 1. Here we provide each rod's physical description, impact velocity and orientation, residual length, and the length of the water filled targets.

Table 1. Summary of Water Column Experiments

NRL TEST NO.	PROJECTILE		IMPACT VELOCITY (km)	CONDITIONS		WATER COLUMN LENGTH (cm)	OBSERVATIONS
	DIA. (cm)	LGTH (cm)		PITCH (degrees)	YAW (degrees)		
2-687	.762	2.291	3.60	2.9 Up	4.6 Left	15	.50 cm residual lgth
2-688	.762	2.289	2.84	0	1 Right	15	.91 cm residual lgth
2-689	.762	2.388	2.32	.8 Down	.5 Right	15	.15 cm residual lgth
2-690	.762	2.388	3.86	2.2 Up	.4 Right	15	.40 cm residual lgth
2-695	.478	7.153	2.66	.7 Down	.67	40	Rod fractured
2-696	.478	7.160	2.26	0	1.6	46	Rod fractured
2-717	.762	2.286	4.57	.5 Up	0	15	No residual lgth
2-718	.475	7.165	2.47	1 Up	2 Right	15	1.0 cm residual lgth
2-719	.762	2.286	4.31	4 Up	0	15	.33 cm residual lgth

It is interesting to note that in experiments 2-695 and 2-696, the tungsten rod fractured as shown below in Figure 3. This fracture was very repeatable. In other experiments, not included in this paper, fracture occurred in each case where the water column exceeded 25 cm.



3a. Rod Launch

3b. Rod Fracture

Figure 3. Test 2-696 – Rod Fracture in Water Column Target

Table 2 summarizes the three experiments performed using the water module configuration.

Table 2. Summary of Three Water Module Experiments

NRL TEST NO.	PROJECTILE		IMPACT VELOCITY (km)	CONDITIONS		MODULE ORIENTATION	OBSERVATIONS
	DIA (cm)	LGTH (cm)		PITCH (degrees)	YAW (degrees)		
2-697	.406	10.15	2.27	.5 Up	.8 Right	13°	1.676cm residual lgth
2-698	.406	15.04	2.24	.3 Up	0	40°	3.302cm residual lgth
2-715	.406	15.24	2.20	0	0	60°	No perforation of fourth module

In these experiments, no rod fracture was observed. Figure 4 shows radiographs from a typical experiment using the water module configuration.



4a. Rod Launch

4b. Penetration of Fourth Module

Figure 4. Sample Results for Water Module

Note that all experiments demonstrated excellent rod control. The projectiles had little pitch or yaw.

CALCULATIONS

Since pitch and yaw were minimal in the water column experiments, most could be modeled using an axisymmetric assumption. The exceptions were the two experiments where the rod fractured. In those experiments, we assumed that the fracture resulted from bending brought on by the projectile's orientation. This meant that a three dimensional treatment was required. Similarly, all the water module experiments required three-dimensional simulation due to the oblique impact.

Figures 5 and 6 summarize the calculations. While the model geometry depended upon the experiment, we chose a standardized treatment of the constitutive and volumetric aspects of the simulations.

Figure 5 shows the problem set-up for the water column analysis. The experiment was modeled using an axisymmetric assumption. The problem size was 50,000 cells, and was run on a Silicon Graphics workstation. The Johnson-Cook constitutive model was used for rods [4]. The water was modeled as a fluid. We chose to use Johnson-Cook damage model for the rods [4]. The model used Mie-Gruneisen equations of state, and the slip interface between the rod and water was approximated using the BLINT option in CTH [5].

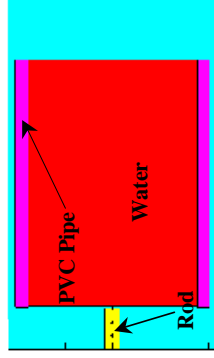


Figure 5. Problem Set-up Water Column Analysis Summary

Figure 6 shows the problem set-up for the water module analysis. The experiment was modeled using 3-D calculations. The problem size was 26 million cells, and was run on a 32 node SGI Origin 2000. The rods were modeled using the Johnson-Cook constitutive and damage models. The target constitutive response was modeled using a hydrodynamic assumption for the water and an elastic-perfectly-plastic constitutive model for all other target materials. The Mie-Gruneisen equation of state was used to describe the volumetric response of both the projectile and the target materials. Note that there is a significant difference between the 2 and 3-D calculations. That difference is a result of the way in which the slip interface between materials is treated. In the 2-D calculations we have used the BLINT option which allows for "sliding" between the materials [5]. This option is not currently available in production versions of the CTH code for 3-D calculations. The effect of BLINT will be discussed more fully in the next section.

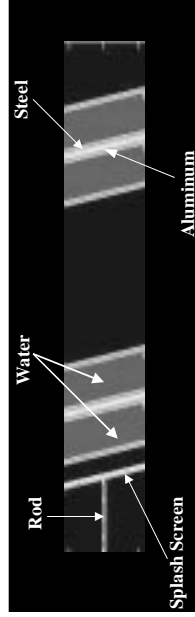
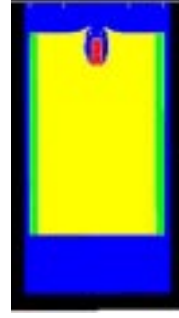


Figure 6. Water Module Analysis Summary

In general, we were able to correctly model the experiments. A typical example is Figure 7, which shows the calculation and radiograph of test 2-688. However, we were unable to reproduce the fracture observed in tests 2-695 and 2-696. Figure 8 shows the results of calculations for test 2-696. The discrepancy between the experiment and calculation is obvious.

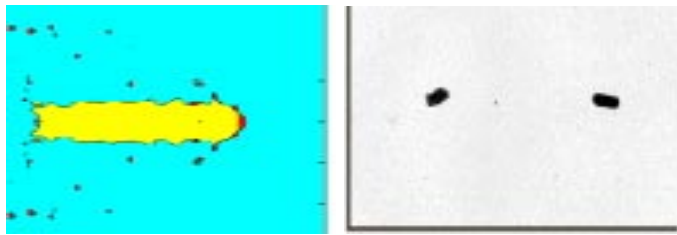


7a. CTH Hydrocode Model



7b. Radiograph of Experiment

Figure 7. Test 2-688—Water Column Experiment



8a. CTH Hydrocode Model

8b. Radiograph of Experiment

Figure 8. Test 2-696 Results – Water Module Experiment

CORRELATION OF NUMERICAL AND EXPERIMENTAL RESULTS

Our objectives in modeling the experiments were to ensure that we could accurately reproduce the erosion and breakup of the tungsten projectiles. Accordingly, our correlation discussion focuses on these two aspects of the study. We begin by looking at the erosion of the projectiles. Figure 9 shows the results when we compare the experimental and numerical results of this study. The results have been normalized by dividing the final projectile lengths by their initial lengths. Those experiments where fracture of the rods occurred are not included. We have included results of several spaced plate experiments, which were simulated using a 3-D model. While these experiments have not been described in this paper, their inclusion allows us to develop meaningful statistical insight into how reality is duplicated by the model.

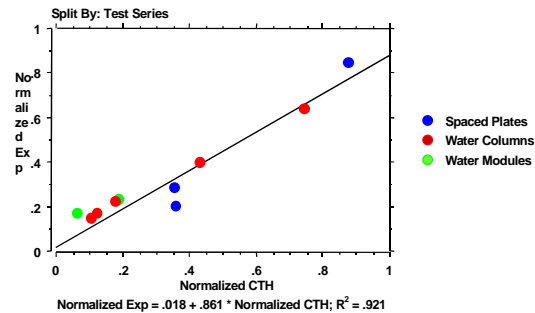


Figure 9. Results for Rod Erosion

As can be seen, the data and calculations correlate well. A linear regression analysis shows an excellent fit. The R^2 value of .921 indicates that only 8% of the variance is unexplained by our fit. Another interesting aspect of the analysis is that the slope of the fit (.861) indicates that CTH is overpredicting the erosion of the projectile by about 14%.

Some insight is gained when we look at Figure 10. Here, we have plotted only the results of our 2-D calculations. The figure shows that these results provide an even better fit to the data; the unexplained

variance is only 4%. Note that the slope has increased to .9005. So, while CTH is still overpredicting erosion, the overprediction has decreased by 4%.

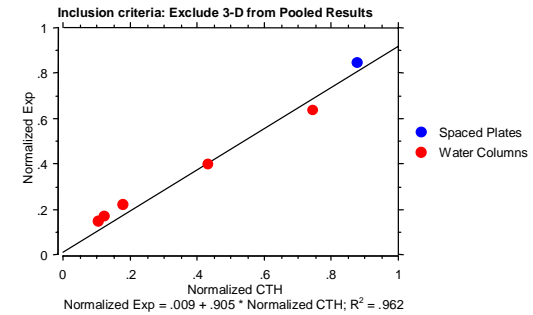


Figure 10. Axisymmetric Results

Figure 11, which shows only 3-D calculations, highlights more dramatic differences. Here, the unexplained variance has increased to 14%. The slope indicates that erosion in CTH is now overpredicted by 25%.

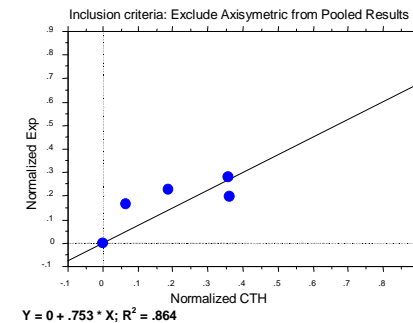


Figure 11. 3-D Results

There are three possible explanations for the discrepancy between the 3-D calculations and the experimental data. The first is problem resolution: the 3-D calculations were not resolved as well as the 2-D calculations. The second is target strength: the steel used in the experiments had a 20% lower yield strength than that assumed in our initial calculations. The third explanation is the slip interface algorithm used: the 2-D calculations used the BLINT algorithm noted earlier, while the 3-D calculations did not incorporate this feature.

In order to evaluate each of these explanations, we developed an axisymmetric analog to the water module experiment shown below in Figure 12. The model is based upon experiment 2-697 where the layers have been scaled by the cosine of 13°.

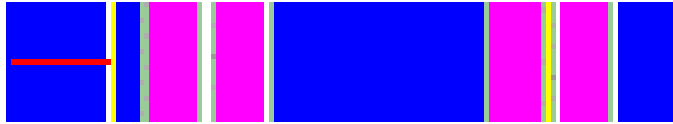


Figure 12. An Axisymmetric Analog to the Water Module Problem

Using this model, we performed studies to examine the effects of resolution, target material strength, and mixed cell interface treatment. The results are shown below in Figure 13. Here, we can see that problem resolution did not affect the results significantly. It is also evident that target material strength had a marginal influence. However, the use of the BLINT option results in a 20% improvement in the agreement between calculated and experimental results. Hence, proper slip interface treatment is essential to successfully predicting rod erosion.

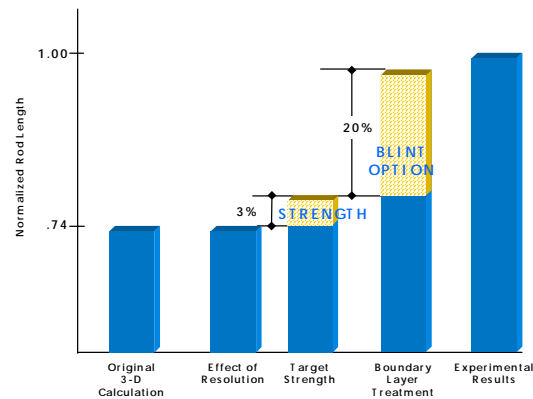


Figure 13. Moving Toward an Answer

In contrast to the predicted erosion, we have no confirmed explanations for our inability to reproduce the rod fracture seen in tests 2-695 and 2-696. Again, problem resolution is a possible explanation. A change in the rod material properties during penetration may also explain the observed fracture. We have performed several calculations to gain insight into the discrepancy. Figure 14 shows the results of a highly resolved calculation of test 2-696. As can be seen, a significant amount of damage has been predicted (a damage value of 1 means the material has failed). Yet, no structural failure is apparent. Also, this calculation incorporates the use of a beta version of the 3-D BLINT algorithm. Since we have replicated the impact conditions, and are properly accounting for the slip interactions, our conclusion is that the rod material is not being properly modeled. To this end, rod material properties are being evaluated using light gas gun and split Hopkinson Bar experiments at the Naval Surface Warfare Center Dahlgren Division. Results of the material investigation are encouraging, but inconclusive, at this time. They indicate a loss of ductility in the tungsten rod material under high strain rate loading [6]. An alternative explanation is that the dynamic failure phenomenon in the rod cannot be represented by a Johnson-Cook model.

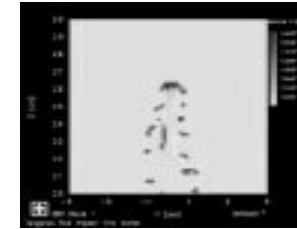


Figure 14. Results of a 3-D Calculation of Test 2-696

CONCLUSIONS

From the results presented in this paper, the following conclusions may be drawn. First, the CTH calculations correlate well with the experimental results in most cases. This agreement is quantitative, as is evident from the correlation plots that show only 8% of the variance is unexplained. Second, proper slip treatment between the rod and water is critical to predicting rod residual lengths. Finally, we have not been successful in reproducing rod fracture. We feel that this may be due to a change in rod material properties and continue to investigate the issue. Therefore, while we acknowledge that the calculations do not perfectly replicate the experiments, they have helped us to understand some of the more unique experimental results.

ACKNOWLEDGEMENTS

The authors would like to acknowledge the following people for their support and help with this task: the late Dr. Andrew Williams who overcame many obstacles to perform the experiments summarized in this paper. Ms. Jeanette Dickens and Jennifer Dickens of Advanced Technology and Research Corp. for editing and graphics support.

REFERENCES

1. Yatteau, Jerome D.; Zernow, Richard H.; Recht, Rodney F., *Compact Fragment Multiple Plate Penetration Model (FATEPEN 2)*, Volume II – Computer Code User's Manual, Applied Research Associates for Naval Surface Warfare Center, Dahlgren, VA January 1991
2. Figures based upon sketches provided to the authors by the late Dr. Andrew Williams.
3. Hertel, E. S. Jr.; Bell, R. L.; Elrick, M. G.; Farnsworth, A. V.; Kerley, G. I.; McGlaun, J. M.; Petney, S. V.; Silling, S. A.; Taylor, P. A.; and Yarrington, L., *CTH: A Software Family for Multi-Dimensional Shock Physics Analysis*, Proceedings of the 19th International Symposium on Shock Waves, Volume 1, pages 377-382, Marseilles, France, 26-30 July 1993
4. Zukas, Jonas A., Editor, *High Velocity Impact Dynamics*, Computational Mechanics Associates, Towson, MD, John Wiley & Sons, Inc., Copyright 1990
5. Silling, Stewart, *An Algorithm for Eulerian Simulation of Penetration*, New Methods Trans Analysis, P. Smolinski, et al., Eds. ASME, PVB Vol 246, pp. 123-129, 1992
6. Unpublished test data developed by L.T. Wilson, Benny Simpson, and Dr. William Holt of NSWCCD.